Contrib Mineral Petrol (2000) 140: 316–327

Wolfgang D. Maier · Nicholas T. Arndt · Edward A. Curl

Progressive crustal contamination of the Bushveld Complex: evidence from Nd isotopic analyses of the cumulate rocks

Received: 5 October 1999 / Accepted: 7 July 2000

Abstract We report the first Nd isotopic data on the cumulate rocks of the Bushveld Complex, South Africa. We analysed 17 whole-rock samples covering 4700 m of stratigraphy through the Lower, Critical and Main Zones of the intrusion at Union Section, north-western Bushveld Complex. The basal ultramafic portions of the complex have markedly higher εNd(T) (−5.3 to −6.0) than the gabbronoritic Main Zone (εNd(T) −6.4 to −7.9). The rocks of the Upper Critical Zone have intermediate values. These results are in agreement with new Nd isotope data on marginal rocks and sills in the floor of the complex that are generally interpreted as representing chilled parental magmas, and with published Sr isotopic data, all of which show a larger crustal component in the upper part of the intrusion. In contrast, the concentrations of many highly incompatible trace elements are decoupled from the isotopic signatures. The basal portions of the complex have higher ratios of incompatible to compatible trace elements than the upper portions. The variations of isotopic and trace-element compositions are interpreted in terms of a change in the nature of the crustal material that contaminated Bushveld magmas. Those magmas that fed into the lower part of the complex had assimilated a relatively small amount of incompatible trace-element-rich partial melt of upper crust, whereas magmas parental to the upper part of the complex had assimilated a higher proportion of the incompatible trace-element-poor residue of partial melting.

W. D. Maier (✉)
Centre for Research on Magmatic Ore Deposits,
Department of Earth Sciences, University of Pretoria,
Pretoria 0002, South Africa
e-mail: wdmaier@scientia.up.ac.za

N. T. Arndt
Géosciences UPR 4661, Université de Rennes,
35042 Rennes cedex, France

E. A. Curl
Department of Earth Sciences, Monash University,
Clayton, Victoria 3168, Australia

Present address:
N. T. Arndt
LGCA, Université de Grenoble, BP 53,
38041 Grenoble cedex, France

Editorial responsibility: I. Parsons

Introduction

The Bushveld Complex of South Africa is the world's largest layered mafic–ultramafic intrusion, with a subsurface outcrop area of ~60,000 km^2. It is also the host of some of the largest deposits of chrome and platinum-group elements. However, despite its petrological and economic importance, its formation is not well understood. Most authors agree that the enormous volume of mafic magma within the complex is best explained by the upwelling of hot mantle, probably a plume from a deep source (Hatton 1995; Hatton and Schweitzer 1995). A longstanding debate continues about whether the unusual chemical characteristics of the Bushveld and associated magmas are related to crustal contamination during ascent or partial melting of enriched mantle lithosphere (Hatton and Sharpe 1989; Harmer and von Gruenewaldt 1991; Buchanan et al. 1999; McCandless et al. 1999). It is also unclear whether the complex was filled through the emplacement of a small number of magma pulses or whether it was an open system through which magmas passed en route to the surface.

To cast some light on these processes, we present the first Nd isotopic data from the cumulate sequence of the Bushveld Complex and some new trace element data from sills in the floor of the complex. We use these data to estimate the compositions of parental magmas, and then try to constrain the magmatic evolution of the complex itself. We will attempt, in particular, to find an explanation for a remarkable change in the composition of parental magmas that characterises not only the Bushveld Complex but also other layered mafic-ultramafic intrusions such as the Stillwater Complex of Montana. Various authors, e.g. Sharpe (1981), Harmer

and Sharpe (1985), Lambert et al. (1994) and Maier and Barnes (1998) have shown that the magmas parental to the lower ultramafic portions of these intrusions share the peculiar combination of high concentrations of incompatible trace elements and strong fractionation of rare earth elements coupled with relatively low initial $^{87}Sr/^{86}Sr$ ratios. In contrast, magmas parental to the main and upper parts of the complexes have lower concentrations of incompatible elements, less fractionated REE but much higher initial $^{87}Sr/^{87}Sr$. This change recalls variations observed in certain sequences of continental flood basalts, in which the lower units of trace-element-enriched 'high-Ti' basalts give way up section to 'low-Ti' basalts with lower trace element contents. In continental basalt provinces, the transition is interpreted to reflect a change in the compositions of mantle source rocks or in the conditions of melting. In flood basalt sequences, however, the pronounced decoupling of trace-element and isotope ratios observed in the mafic–ultramafic complexes appears to be absent: the basalts with the most highly fractionated REE generally have the most radiogenic Sr isotope compositions.

In this paper we will show that by combining information from layered intrusions and volcanic sequences it is possible to build a better picture of the complex history of mantle melting and crustal contamination that governs the evolution of continental high-volume basaltic provinces.

Stratigraphy of the Bushveld Complex

The layered sequence of the Bushveld Complex is generally subdivided into Marginal, Lower, Critical, Main, and Upper Zones (Fig. 1; Eales and Cawthorn 1996). At Union Section, the 800-m-thick Lower Zone consists predominantly of olivine-bearing ultramafic cumulates, whereas the overlying Lower Critical Zone of similar thickness is dominated by orthopyroxenites. The base of the 400-m-thick Upper Critical Zone is defined by the appearance of cumulus plagioclase resulting in the occurrence of norites and anorthosites in addition to orthopyroxenites and harzburgites. Both Lower and Upper Critical Zones host up to 13 massive chromitite layers of up to 1.6 m in thickness (Fig. 2). A number of sulphide-bearing ultramafic layers are found towards the top of the Upper Critical Zone. Some of these, notably the Merensky Reef, are highly enriched in platinum-group elements (PGE). The Main Zone is a 2- to 3-km-thick sequence of relatively uniform gabbro–norites. The 1.5-km Upper Zone, which has not been studied by us, is broadly ferrodioritic and hosts up to 25 layers of economically important massive vanadiferous magnetite.

Previous ideas on the evolution of the complex

Generalized major- and trace-element differentiation trends through the sequence were shown in Eales and Cawthorn (1996) and Maier and Barnes (1998). The prominent modal and compositional layering of the complex is generally explained by a combination of magma fractionation and replenishment of the chamber (Kruger 1994; Eales and Cawthorn 1996). The main evidence comes from variations in mineral compositions. The Mg* [molar MgO/(MgO + FeO)] and Cr contents of orthopyroxenes generally

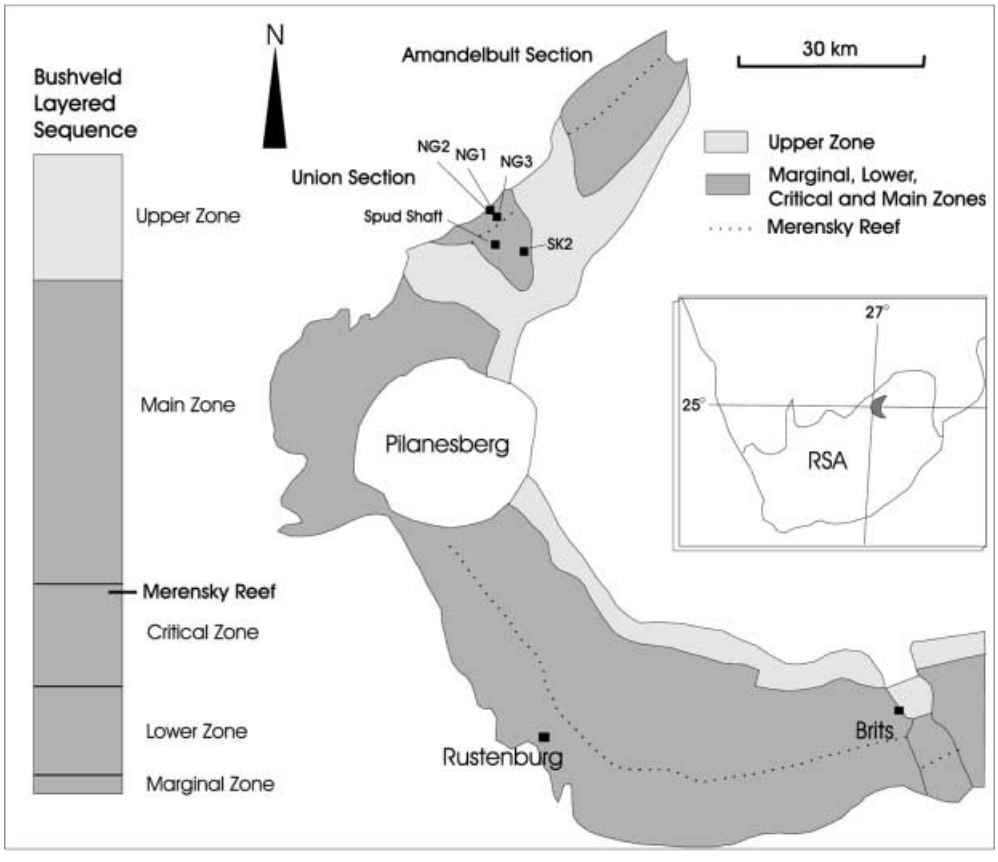

Fig. 1 Map of the Western Bushveld Complex showing location of borehole sites, and simplified stratigraphic column of the Rustenburg Layered Suite

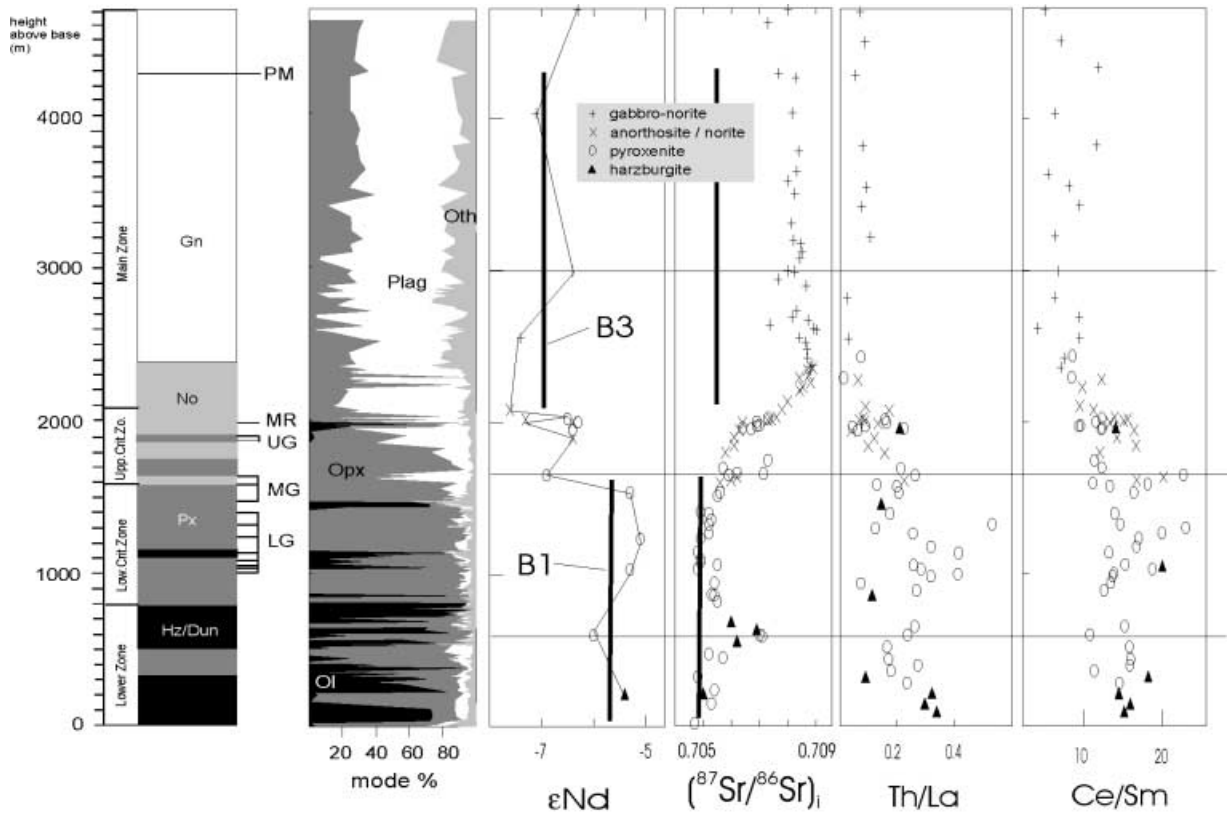

Fig. 2 Mineral modes, εNd (2060 m.y.), $^{87}Sr/^{86}Sr_i$ (2060 m.y.), Th/La, and Ce/Sm, plotted as a function of height in the studied interval. The modal and Sr isotopic data are from Mitchell (1986), Eales et al. (1990), de Klerk (1992), and Teigler and Eales (1996), and the trace-element data from Maier and Barnes (1998)

decrease from high values in the Lower and Lower Critical Zones to much lower values in the Upper Zone, but numerous reversals of the general trend occur at scales of centimetres to hundreds of metres. Similar differentiation trends are found in chromite and olivine, but reversals in plagioclase compositions are less prominent.

Until the late 1970s, it was assumed that the compositional evolution of the chamber was best explained by progressive differentiation of a single parental magma. However, the advent of isotopic studies demonstrated that the complex crystallised from magmas that contained a progressively larger component from a geochemically enriched source, as indicated by Sr (Hamilton 1977; Harmer and Sharpe 1985; Kruger 1994), Pb (Harmer et al. 1995), and Os (Schoenberg et al. 1998; McCandless et al. 1999) isotope data. Although some authors (e.g. Harmer and Sharpe 1985) assumed that the enriched component came from the lithospheric mantle, many others concluded that this component was old continental crust. The predominance of orthopyroxene over clinopyroxene in the ultramafic portions of the intrusion has been linked to the assimilation of siliceous crustal rocks (Irvine 1970; Sparks 1986). It was further suggested that the appearance of plagioclase on the liquidus at the base of the Upper Critical Zone may represent the intrusion and in-mixing of magmas whose compositions fell in the primary stability field of plagioclase, rather than representing cotectic crystallisation of plagioclase and pyroxene from differentiating basaltic magma (Sharpe and Irvine 1983).

Based on the compositions of sills and marginal rocks in the floor of the complex, Sharpe (1981) and Harmer and Sharpe (1985) proposed that the complex crystallised from three different magma types. A magnesian basalt (referred to as B1 or U-type magma) with the crystallisation order ol–opx–plag (Sharpe and Irvine 1983), gave rise to the ultramafic Lower and Lower Critical Zones. An aluminous tholeiite (B3 or A-type) with the crystallisation order plag–ol–cpx–opx (Sharpe and Irvine 1983) yielded the gabbroic Main Zone, and B2, roughly intermediate between the two other magmas, yielded the predominantly noritic Upper Critical Zone. New estimates of the compositions of B1 and B3, based on an ongoing study by E. Curl, are listed in Table 1. The B1 estimate is

Table 1 Estimated composition of B1 and B3 magmas (data from Curl, in preparation)

	B1 $n = 3$	B3 $n = 7$
Fe_2O_3 (%)	10.24	10.62
MnO (%)	0.18	0.19
TiO_2 (%)	0.36	0.46
CaO (%)	6.89	10.95
K_2O (%)	1.12	0.34
P_2O_5 (%)	0.09	0.05
SiO_2 (%)	56.74	51.58
Al_2O_3 (%)	13.06	16.04
MgO (%)	9.00	7.57
Na_2O (%)	1.89	1.85
Selected ICP-data (ppb)		
Ce	41,419	16,456
Cr	485,887	459,511
La	21,455	8,036
Nd	18,142	8,702
Ni	169,419	135,170
Rb	42,917	11,147
Sm	3,338	2,073
Sr	242,714	335,103
Th	4,380	845
Yb	1,173	1,192
Zr	97,749	30,740

derived from three samples of fine-grained diabase showing well-defined chill textures ('cone diabase' of Sharpe 1978). This composition differs from earlier, more magnesian, estimates of B1 (Harmer and Sharpe 1985), which were based on a larger population of micropyroxenites. The new data show that the more magnesian pyroxenites probably contain a significant component of cumulus pyroxene and lesser amounts of olivine (Curl in preparation). The B3 estimate is derived from seven samples of gabbroic sills.

Decoupling of trace-element ratios from isotope concentrations is seen in the data of Mitchell (1986), de Klerk (1992), Kruger (1994), Teigler and Eales (1996), and Maier and Barnes (1998), plotted in Fig. 2. The lower portions of the Bushveld Complex have initial Sr isotope ratios ($^{87}Sr/^{86}Sr_i$) that are relatively low compared with those of the upper portions of the complex. However, the same rocks have markedly higher ratios of incompatible to compatible elements (Figs. 2 and 3 and Table 1). Thus we find low $^{87}Sr/^{86}Sr_i$ (0.705–0.707) coupled with high ratios of Ce/Sm (10–23) and Th/La (0.1–0.5) in the Lower Zone, and high $^{87}Sr/^{86}Sr_i$ (0.707–0.709) coupled with low ratios (Ce/Sm 4–12, and Th/La 0.1) in the Main Zone. The B1 and B3 magmas show similar trends (Fig. 2). This pattern is in marked contrast with what is seen in smaller layered intrusions, such as Skaergaard (Stewart and de Paolo 1990) or layered units in the Cape Smith Belt (e.g. Francis and Hynes 1979) where the upper more differentiated rocks tend to have relatively high ratios of highly incompatible to compatible trace elements.

Analytical methods

The present study is largely based on drill cores from the Union Section of Rustenburg Platinum Mines, which comprise a 4700-m-long section from the base of the layered suite to the top of the Main Zone. The location of the boreholes is shown in Fig. 1. Sample S11 was collected from the side wall of the Spud Shaft of the mine, and sample MZ7 is a surface sample. Detailed lithological, petrographic and geochemical descriptions can be found in the original work of Eales et al. (1990), Mitchell (1986), de Klerk (1992), Kruger (1994), and Teigler and Eales (1996). More recent papers present the concentrations of rare earth elements (Maier

Table 2 Major element (in wt%) data on the analysed samples (data from Mitchell 1986; De Klerk 1992; Teigler and Eales 1996; Maier and Barnes 1998). All data are recalculated to 100% LOI-free. Fe_2O_3 has been stated assuming a constant ratio of FeO/Fe_2O_3 = 10. *Height* height above base of complex. *Hz* Harzburgite; *Px* pyroxenite; *No* norite; *An* anorthosite; *Gn* gabbronorite

Sample	Rock type	Height	SiO_2	TiO_2	Al_2O_3	FeO	Fe_2O_3	MnO	MgO	CaO	Na_2O	K_2O
MZ 7	Gn	4712	51.76	0.17	16.33	6.47	0.64	0.15	10.16	12.46	1.70	0.14
A 1	Gn	4032	52.83	0.13	19.61	5.85	0.59	0.14	5.73	12.03	2.89	0.19
A 168	Gn	2994	51.76	0.13	17.94	5.39	0.54	0.13	8.66	13.33	1.99	0.13
A 254	Gn	2555	51.63	0.17	17.59	6.03	0.60	0.11	10.32	11.74	1.60	0.20
UA 2	An	2082	50.22	0.12	28.04	2.32	0.23	0.03	2.38	14.00	2.38	0.26
UA 25	Px	2024	54.92	0.20	5.30	9.67	0.97	0.21	24.33	3.59	0.70	0.10
UA 31	An	2019	48.20	0.04	31.66	0.86	0.09	0.01	1.25	15.41	2.29	0.20
UA 41	Px	2002	54.62	0.26	5.68	9.57	0.96	0.20	23.47	4.19	0.79	0.22
UA 48	An	1994	49.41	0.07	29.29	1.66	0.17	0.03	1.70	15.11	2.34	0.16
B 235/36	Px	1955	53.22	0.18	4.87	11.80	1.18	0.26	25.04	3.75	0.71	0.09
S 11	No	1900	53.02	0.11	11.49	8.03	0.80	0.18	18.83	6.19	1.23	0.08
NG3 159.4	Px	1654	52.20	0.20	5.00	10.90	1.10	0.20	24.40	3.20	0.50	0.10
NG1 25	Px	1538	55.30	0.20	3.60	10.60	1.10	0.20	24.80	3.20	0.40	0.00
NG1 327.45	Px	1236	55.20	0.10	2.90	9.40	0.90	0.20	27.50	2.60	0.30	0.00
NG1 528.5	Px	1035	54.70	0.10	3.00	8.70	0.90	0.20	28.40	2.20	0.40	0.00
NG2 171.5	Px	602	54.60	0.10	2.20	9.20	0.90	0.20	30.10	1.70	0.20	0.00
NG2 557.1	Hz	216	53.70	0.10	3.00	9.00	0.90	0.20	29.50	2.20	0.60	0.10

Table 3 Trace element (in ppm) data on the analysed samples (data from Mitchell 1986; De Klerk 1992; Teigler and Eales 1996; Maier and Barnes 1998). *Height* height above base of complex. *Hz* Harzburgite; *Px* pyroxenite; *No* norite; *An* anorthosite; *Gn* gabbronorite

Sample	Rock type	Height	Cr	Ni	Rb	Sr	Zr	Th	La	Ce	Yb	Mg# wr
MZ 7	Gn	4712	359	188	2	220	8	0.17	2.38	3.85	0.55	0.74
A 1	Gn	4032	14	92	3	322	5	< 0.1	2.24	3.80	0.42	0.64
A 168	Gn	2994	59	193	1	243	9	< 0.1	2.42	5.24	0.54	0.74
A 254	Gn	2555	356	233	4	222	7	0.09	2.85	6.71	0.57	0.75
UA 2	An	2082	118	39	3	340	15	0.77	4.46	7.73	0.33	0.63
UA 25	Px	2024	2678	845	18	74	17	0.51	3.27	7.75	0.57	0.80
UA 31	An	2019	49	55	4	397	4	0.16	2.30	3.74	0.08	0.71
UA 41	Px	2002	2929	736	8	66	22	0.96	5.89	13.27	0.75	0.80
UA 48	An	1994	66	29	5	463	9	0.36	2.66	5.48	0.19	0.63
B 235/36	Px	1955	3310	572	< 1	55	8	0.12	1.90	5.61	0.51	0.79
S 11	No	1900	1990	390	1	164	7	0.17	1.40	3.56	0.27	0.79
NG3 159.4	Px	1654	14263	549	4	53	10	0.34	1.29	5.81	0.35	0.80
NG1 25	Px	1538	4140	497	3	33	10	0.40	1.95	6.71	0.55	0.81
NG1 327.45	Px	1236	5700	480	2	19	5	< 0.1	1.14	4.90	0.32	0.84
NG1 528.5	Px	1035	8202	497	2	29	7	0.30	1.07	4.12	0.16	0.85
NG2 171.5	Px	602	3308	723	1	18	5	0.29	1.24	3.22	0.25	0.85
NG2 557.1	Hz	216	4078	745	5	43	18	0.50	1.54	3.91	0.19	0.85

and Barnes 1998) and platinum-group elements (Maier and Barnes 1999). The newly analysed samples represent all major rock types of the sequence, including harzburgite, orthopyroxenite, norite, gabbronorite, and anorthosite. Selected whole-rock data of the samples are listed in Tables 2 and 3.

We measured the Nd isotope compositions of 17 samples and Sr isotope compositions of four samples. The initial Sr isotopic ratios for a further five samples are from Mitchell 1986, Eales et al. 1990, de Klerk 1992, and Teigler and Eales 1996, and those for the remaining eight samples are extrapolated from an adjacent borehole (Eales et al. 1990). The analyses were carried out at the University of Rennes using standard techniques as outlined by Arndt et al. (1998). Results were normalised to $^{88}Sr/^{86}Sr = 8.375209$ and $^{146}Nd/^{144}Nd = 0.7219$. Semi-dynamic measurements of the in-house standard Rennes–Ames gave an average of 0.511965 ± 6 (2 s, 50 measurements) corresponding to a $^{143}Nd/^{144}Nd$ of 0.511856 for La Jolla standard. No correction was applied to the measured values. Total blanks were 100 pg for Nd and 60 pg for Rb.

Results

Epsilon Nd (T) and initial $^{87}Sr/^{86}Sr_i$ ratios calculated for an age of 2060 m.y. (Walraven et al. 1990) are listed in Table 4. In Fig. 2, $\varepsilon Nd(T)$, $^{87}Sr/^{86}Sr_i$ as well as Ce/Sm and Th/La ratios are plotted against stratigraphic height and mineral modes. In general, $\varepsilon Nd(T)$ decreases and $^{87}Sr/^{86}Sr_i$ increases with stratigraphic height in the complex. The Lower and Critical Zones have $\varepsilon Nd(T)$ of between −5.3 and −6.0 and $^{87}Sr/^{86}Sr_i$ between 0.705 and 0.707, whereas the Main Zone has $\varepsilon Nd(T)$ between −6.4 and −7.9 and $^{87}Sr/^{86}Sr_i$ of 0.708 and 0.709. It is evident from Figs. 2 and 3 that there is a negative correlation between $^{87}Sr/^{86}Sr_i$ and $\varepsilon Nd(T)$, even on a small scale, as illustrated at the distinct isotopic breaks within the Lower Zone, below the MG4 chromite and in the central Main Zone. Superimposed on the general trend are several reversals, notably in the Bastard pyroxenite (Fig. 4).

New average isotope compositions of the B1 and B3 magmas (data from Curl, in preparation) are also plotted into Fig. 2. They mostly show a good correlation with the cumulates of the Bushveld Complex. The B1 magmas, which are thought to represent the magmas parental to the Lower Zone, have low $^{87}Sr/^{86}Sr_i$ but high $\varepsilon Nd(T)$, and the B3 magmas, which are equated with the Main Zone, have high $^{87}Sr/^{86}Sr_i$ and low $\varepsilon Nd(T)$. It is notable, however, that $^{87}Sr/^{86}Sr_i$ ratios in the cumulates of the complex tend to be higher than in the sill rocks: values > 0.7065, which are common in the cumulates, are absent from the sills.

The parallel behaviour of Nd and Sr isotopic compositions demonstrate that the Sr isotopic signature of the Bushveld Complex has not been greatly modified by hydrothermal mobility of Rb or Sr, as may have been implied by the isotopic disequilibrium between different phases documented by Eales et al. (1990). The absence from the sills of the component in the cumulates with high $^{87}Sr/^{86}Sr_i$ and low $\varepsilon Nd(T)$ may indicate that sampling of the B3 sills was unrepresentative or that the B3 sills are not parental to the Main Zone cumulates.

These variations indicate that there was a progressive change in the nature of the liquid that intruded the

Table 4 Neodymium and strontium isotope data. Epsilon Nd and initial $^{87}Sr/^{86}Sr$ values calculated for an age of 2.06 Ga; Sr isotope values reported without measured values are from Eales et al. (1990), Teigler and Eales (1996), de Klerk (1992), and Mitchell (1986)

Sample no.	Zone	Height (m)	Rock type	Nd (ppm)	Sm (ppm)	$^{147}Sm/^{144}Nd$	$^{143}Nd/^{144}Nd$ (Measured)	Error (2 s)	ε_{Nd} (T = 2.06 Ga)	$^{87}Rb/^{86}Sr$	$^{87}Sr/^{86}Sr$ (Measured)	Error (2 s)	$^{87}Sr/^{86}Sr$ (Initial)
NG2 557.1	LZ	216	Hz	1.85	0.38	0.1250	0.511393	8	−5.4	0.247	0.711759	7	0.7044
NG2 171.5	LZ	602	Px	0.85	0.195	0.1388	0.511549	10	−6.0	0.377	0.718591	6	0.7074
NG1 528.5	LCZ	1035	Px	1.47	0.32	0.1297	0.511462	6	−5.3				0.7048
NG1 327.45	LCZ	1236	Px	0.95	0.21	0.1329	0.511513	9	−5.1				0.7049
NG1 25	LCZ	1538	Px	1.94	0.42	0.1306	0.511472	6	−5.3				0.7056
NG3 159.4	UCZ	1654	Px	1.85	0.42	0.1364	0.511468	6	−6.9				0.7059
S 11	UCZ	1900	No	1.29	0.28	0.1313	0.511428	12	−6.4				0.7061
B 235/36	UCZ	1955	Px	2.25	0.53	0.1431	0.511589	7	−6.4				0.7067
UA 48	UCZ	1994	An	2.02	0.38	0.1132	0.511182	7	−6.4				0.7064
UA 41	UCZ	2002	Px	6.68	1.34	0.1212	0.511293	6	−6.3				0.7069
UA 31	UCZ	2019	An	1.57	0.27	0.1033	0.511000	10	−7.3				0.7074
UA25	UCZ	2024	Px	3.24	0.70	0.1301	0.511403	6	−6.5				0.7073
UA2	UCZ	2082	An	4.47	0.87	0.1176	0.511180	9	−7.6				0.7078
A 254	MZ	2555	Gn	3.47	0.85	0.1483	0.511604	6	−7.4				0.7084
A 168	MZ	2994	Gn	3.22	0.82	0.1532	0.511725	9	−6.4	0.013	0.708935	7	0.7085
A1	MZ	4032	Gn	2.39	0.61	0.1535	0.511694	9	−7.1				0.7082
MZ 7	MZ	4712	Gn	3.06	0.80	0.1580	0.511792	5	−6.3	0.033	0.70803	8	0.7070

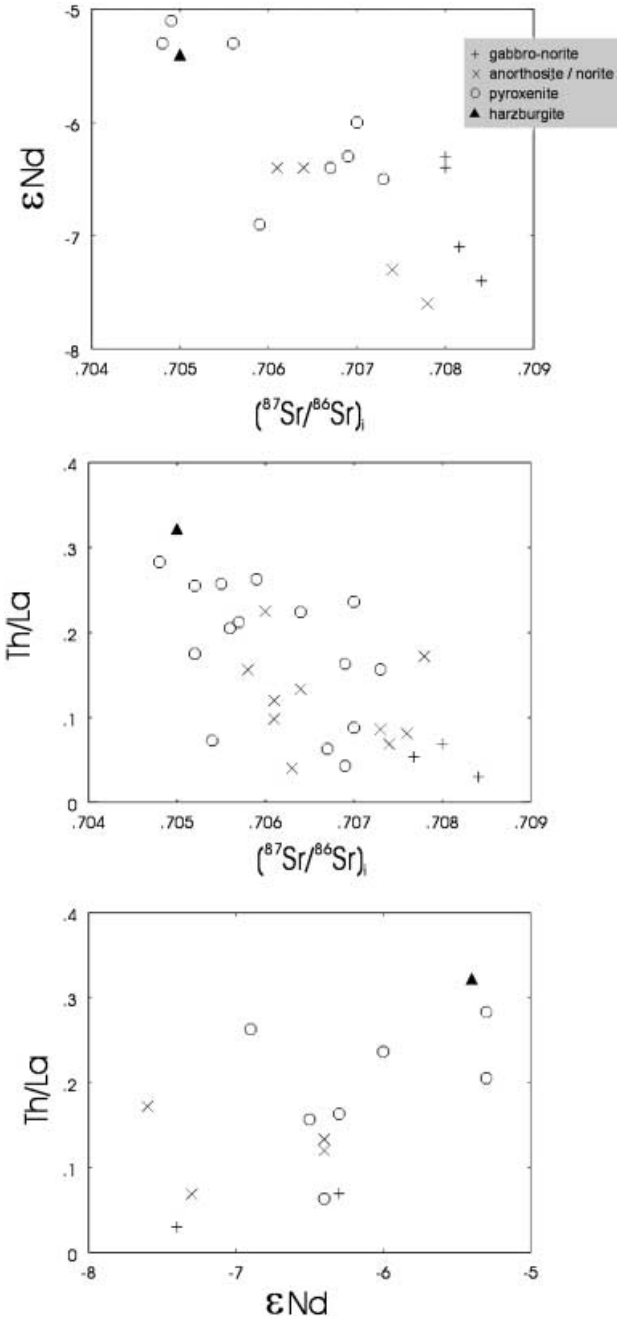

Fig. 3 Binary variation diagrams of **a** εNd(T) versus $^{87}Sr/^{86}Sr_i$, **b** Th/La versus $^{87}Sr/^{86}Sr_i$, and **c** Th/La versus εNd(T)

Bushveld magma chamber. At the early stages, during crystallisation of the Lower Zone and the base of the Critical Zone, this magma had high concentrations of incompatible trace elements, high ratios of incompatible to compatible elements, combined with low $^{87}Sr/^{86}Sr_i$ and high εNd(T). In the Main Zone, the characteristics are reversed: concentrations and ratios of incompatible elements are low, $^{87}Sr/^{86}Sr_i$ is high and εNd(T) is low. These variations are opposite to what is usually seen in magmatic systems: normally a magma with fractionated trace-element ratios (e.g. high Rb/Sr or low Sm/Nd) would have high $^{87}Sr/^{86}Sr_i$ and low εNd(T).

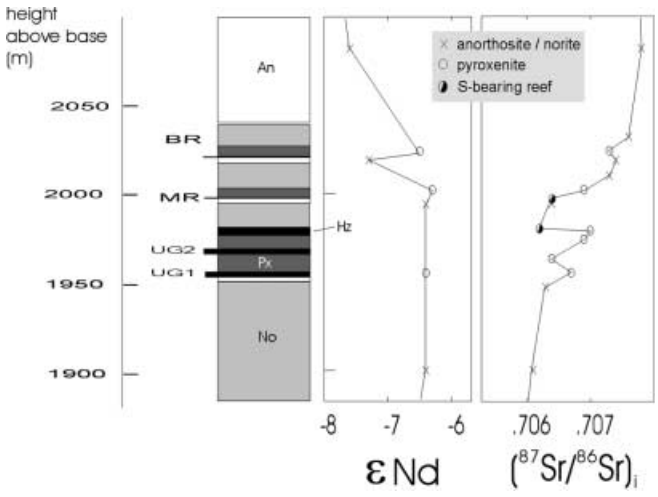

Fig. 4 Epsilon Nd and $^{87}Sr/^{86}Sr_i$ plotted as a function of height in the interval from the foot wall of the UG1 chromitite to the hanging wall of the Bastard Reef

Discussion

The nature and source of the enriched component: modelling crustal contamination

We will show in this paper that the distinctive trace-element and isotopic compositions of Bushveld magmas are mainly the consequence of crustal contamination. We are well aware that many authors prefer an alternative model in which the enrichment in incompatible trace elements and isotopic compositions is attributed to a source in the continental lithospheric mantle, but we feel that the opposing points of view have been sufficiently debated in the literature (e.g. Lassiter and DePaolo 1997, and references therein). It is more constructive to focus on the changing nature of the contamination during the course of the Bushveld event.

In Fig. 5 comparison is made between the average incompatible element compositions of B1- and B3-type sills and literature estimates of the compositions of average lower and upper continental crust. There is a remarkable similarity between incompatible element ratios in B1 sills and those of average upper crust proposed by Taylor and McLennan (1985), particularly in the relative enrichment of the more incompatible elements, the presence of negative Nb–Ta and Ti anomalies, and the absence of a positive Sr anomaly. In contrast, the incompatible element characteristics in B3-type sills resemble those estimated for the lower crust (Rudnick and Fountain 1995), in that both have a less fractionated pattern (lower La/Yb), a less-pronounced Ti anomaly and a distinctive positive Sr anomaly. On the basis of this comparison, it is tempting to propose that the magmas parental to the lower part of the Bushveld Complex were contaminated with material from the upper crust, and those parental to the upper part were contaminated with a large amount of material from the

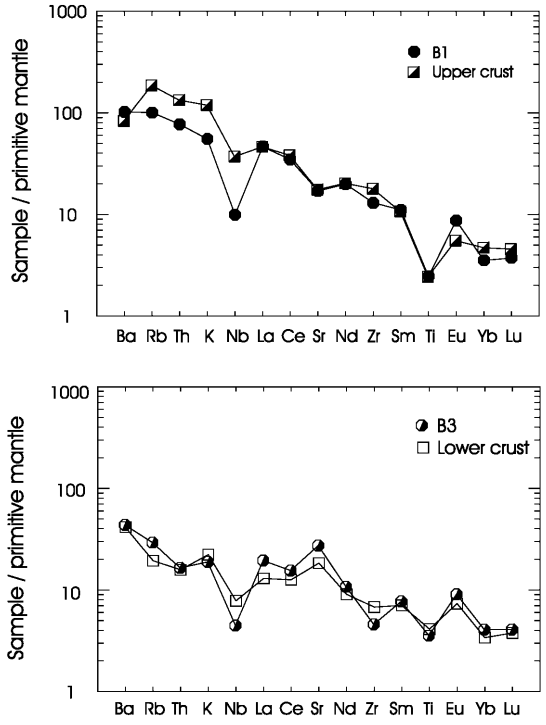

Fig. 5 Comparison between the average compositions of B1- and B3-type sills and estimations of the compositions of lower and upper continental crust (from Rudnick and Fountain 1995). Mantle normalization factors are from Sun and McDonough (1989)

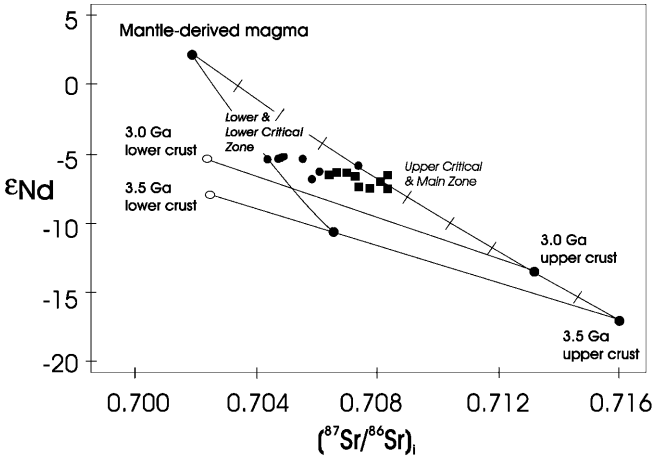

Fig. 6 Diagram of εNd vs $^{87}Sr/^{86}Sr_i$, showing measured compositions of rocks from the Bushveld Complex, an estimated composition of uncontaminated parental magma, and the calculated compositions of rocks from the Kaapvaal Craton at the time of emplacement of the Complex. The parental magma has an isotope composition between that of depleted mantle at 2.1 Ga ($\sim +5$) and bulk earth, as would be expected for magma from a mantle plume (compare with the values in Cretaceous oceanic plateaus ($\sim +5$), which fall between $+12$ and 0). The crustal rocks had the same isotope composition when emplaced but subsequently evolved with the Rb/Sr and Sm/Nd ratios of Taylor and McLennan's (1985) upper crust and Rudnick and Fountain's (1995) lower continental crust. Mixing lines were calculated assuming 52 ppm Sr and 3.4 ppm Nd in the parental picritic magma (Arndt et al. 1993); concentrations in the crustal contaminants are from Taylor and McLennan (1985) and Rudnick and Fountain (1995)

lower crust. Consideration of the isotope data shows, however, that this was not the case.

The key to interpreting the contamination is the decoupling of trace-element and isotopic compositions. In the Kaapvaal craton (which hosts the Bushveld Complex) the maximum age of continental crust is ~3.5 Ga and there are considerable volumes of granite with ages as young as 3.0 Ga (e.g. de Wit et al. 1992). At the time of emplacement of the Bushveld Complex (2.06 Ga ago) material from the upper and lower crust with ages between 3.0 and 3.5 Ga would have had the compositions shown in Fig. 6. The parameters used to calculate these compositions are given in the caption. In the 900 to 1400 m.y. that elapsed between formation of the crust and emplacement of Bushveld magmas, the upper crust would have evolved to high $^{87}Sr/^{86}Sr$ and low εNd but the lower crust, which has far lower Rb/Sr, would have retained a Sr isotopic composition not far removed from that of its mantle source. Although the mixing lines shown in the figure suggest that the rocks of the Bushveld Complex could have formed through contamination of mantle-derived magma with crust of appropriate isotopic composition, consideration of the trace-element data shows that the model does not work. To explain the isotopic composition of the upper part of the complex (i.e. the Main Zone) requires an upper crustal contaminant with highly radiogenic Sr, but the trace-element characteristics of the Main Zone are unlike those of the upper crust and very similar to those of the lower crust. To explain the isotopic characteristics of the lower part of the complex (i.e. the Lower Zone and Lower Critical Zone) whose trace-element patterns resemble upper crust, a contaminant with an isotopic composition more like that of lower crust is required.

An alternative model has been proposed by Sharpe et al. (1986). In an attempt to explain the contrasting trace-element and isotopic characteristics of the lower and upper parts of both the Bushveld and Stillwater Complexes, these authors suggested that the two magma types may have resulted from assimilation of crustal material whose composition changed during the course of the magmatic event. Rather than considering contaminants from different parts of the crust, Sharpe et al. (1986) proposed that the composition of the contaminant changed progressively as a direct result of interaction with the magma parental to the complex. They envisaged the operation, beneath the Bushveld Complex, of a feeder chamber fed by picritic magmas hot enough to cause partial melting in the wall rocks. In the first stage of the process, low-temperature partial melts contaminated the early magmas (see also Francis 1994; Kerr et al. 1995), which then migrated into the overlying chamber where they crystallised to form the lower part of the complex. This partial melt was strongly enriched in incompatible elements and a relatively small proportion was sufficient to cause major changes in the trace-element patterns of the hybrid magma. The effect on the isotopic composition, on the other hand, was relatively

small. Notably, based on field and geochemical evidence, Sharpe et al. (1986) and other authors (e.g. Harmer et al. 1995) generally discard the possibility of significant in situ contamination of the Bushveld magmas.

The progressive contamination has been modelled quantitatively for various crustal end-members using isotope (Fig. 7) and trace element (Fig. 8) data. In view of the uncertainties surrounding the compositions of magma and contaminants, and the complexity of the processes involved, this modelling does not yield unambiguous solutions. Considerable latitude surrounds the selection of the composition of magma produced by melting beneath the Kaapvaal lithosphere, which could have varied from picritic to komatiitic, depending on the thickness of the lithosphere and the temperature and composition of the mantle source. The assimilation of

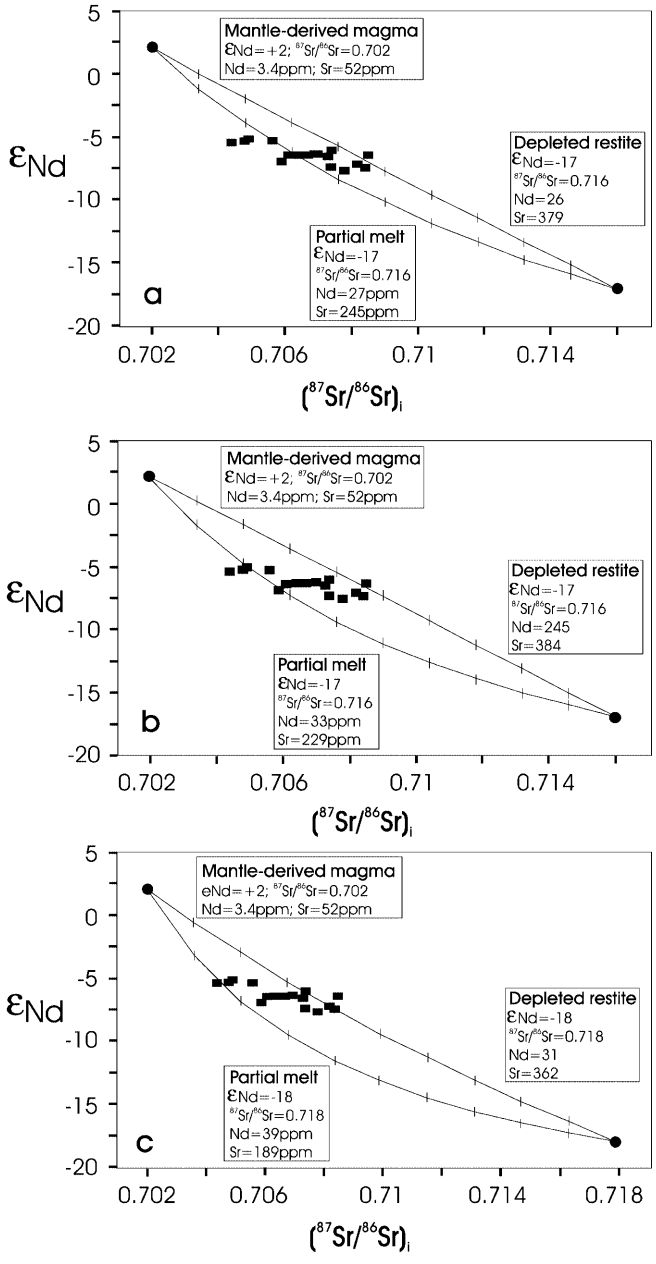

Fig. 7 Diagrams of εNd vs $^{87}Sr/^{86}Sr_i$, showing how the isotope compositions of the lower portion of the Bushveld Complex can be explained by contamination of mantle magma with **a** 5%, and **b** 12% partial melt of upper continental crust, and those of the upper portions by contamination with the refractory residue of partial melting. Cumulates of the Critical Zone plot between the Lower and Main Zones. **c** Crustal end-member is Vredefort lower crust. See text for details

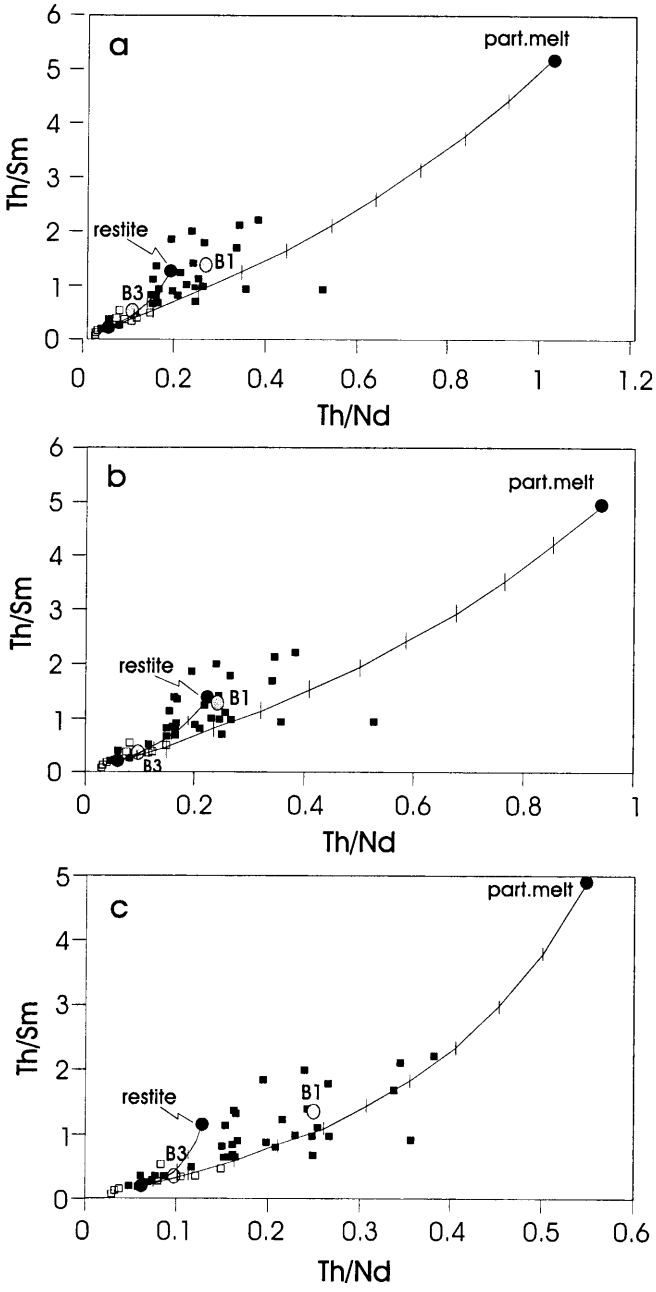

Fig. 8 Diagrams of Th/Sm versus Th/Nd. Bushveld Lower and Critical Zone cumulates (*solid squares*) and B1 magma fall on mixing lines between mantle magma and **a** 5% partial melt of upper crust (at 7 kbar), **b** 12% partial melt of upper crust (at 5 kbar), and **c** 15% partial melt (at 10 kbar) of Vredefort lower crust. Bushveld Main Zone cumulates (*open squares*) are mixtures between mantle magma and the crustal residues. See text for further details

large amounts of crustal rock into such highly magnesian magmas yields hybrid magmas of basaltic composition. The choice of possible assimilant compositions also is large, as illustrated by the discussion in the following paragraphs. However, the major source of uncertainty stems from the mechanism chosen to model the evolution of a magma that assimilates its wall rocks. In many papers, crustal contamination is modelled using bulk mixing, a process that is far from reality and that provides few concrete constraints. Assimilation accompanied by crystallisation (AFC, DePaolo 1981) is more realistic, but it too cannot be applied rigorously to actual magma chambers, which probably function as open systems. To model such systems requires a more complicated approach (O'Hara and Mathews 1981) that introduces additional variables, particularly the flux of magma into and out of the chamber. The large number of variables, combined with uncertainties about end-member compositions, the crystallising assemblages and partition coefficients, provides such a degree of flexibility to the modelling that the composition of virtually any hybrid magma is readily reproduced – the approach is more realistic but it provides few concrete constraints. Given this situation, we have chosen to illustrate our concept of changing contaminant composition using the simplest approach – bulk mixing – recognising that the results cannot be applied quantitatively. We focussed our attention on the nature of the contaminant and the effect this has on the composition of the hybrid magmas. In such an approach, variations in the ratios of isotopes and trace elements retain some significance, but the concentrations of these elements will not be realistic. Similarly, the major element composition, which is controlled mainly by the nature and proportions of minerals that fractionate within the magma chamber, may not necessarily be reproduced.

In Fig. 7a, b the crustal rocks were assumed initially to have the composition of 3.5 Ga upper continental crust with trace element compositions of Taylor and McLennan (1985), except for the lower Nb proposed more recently by Condie (1993) and Plank and Langmuir (1998). The composition of 5 (Fig. 7a) and 12% (Fig. 7b) partial melts of the rocks and the resulting residues were estimated using the experimental data on the melting of biotite gneiss of Patiño Douce and Beard (1995), following the procedure of Rudnick and Presper (1990). Dehydration melting of the upper crustal wallrocks resulted in the formation of a granitic melt with high concentrations of incompatible elements, and a residue strongly enriched in plagioclase. The addition of a relatively small proportion of this contaminant, representing 20% by weight of the lower parts of the complex, is sufficient to explain the observed pattern (Fig. 7a, b).

In Fig. 7c, we used the lower portion of crust exposed in the Vredefort impact structure, which is unusually enriched in incompatible trace elements, as the crustal end-member in the mixing calculations (Hart et al. 1981, 1990). Recalculated to 2060 m.y. and assuming 15% partial melting at 10 kbar (Patiño Douce and Beard 1995), this also provides a reasonable fit. The published data for Vredefort upper crust gave a poor fit mainly because they are too radiogenic (Hart et al. 1981).

The plagioclase-rich residue left after extraction of the low-melting fraction was depleted in Rb, Th and light rare earth elements (LREE) and had a flatter REE pattern. However, it was relatively enriched in Sr and Eu because of its high plagioclase content. These features are the trace-element characteristic of the Main Zone of the complex and of B3 sills (Harmer and Sharpe 1985; Maier and Barnes 1998). Continued interaction between magma in the 'staging chamber' and its wallrocks resulted in relatively large amounts of contamination and the formation of a hybrid magma with the trace-element composition of the upper part of the complex. Because of the high Sr content of the contaminant, the change in Sr isotope composition was particularly large; because of the low Nd content, the effect on Nd was less pronounced. Our modelling indicates that ~40–50% by weight of the Main Zone is composed of upper crustal residue (Fig. 7a, b). This figure is large, but not unreasonable if the wallrocks had been heated to their melting temperature during the first stage of interaction and if the staging chamber operated as an open system.

Our model is in agreement with variations in trace element ratios of Th/Sm vs Th/Nd in B1 and B3 magmas (Fig. 8a–c). The Lower Zone cumulates and B1 magma plot close to a mixing line between mantle melt and partial melts of upper crust, whereas the Main Zone cumulates and B3 magma can be interpreted as mixtures between mantle melt and upper crustal residue. For the Lower Zone cumulates and B1, between 10 and 30% contamination with a small degree (5%) partial melt of upper crust is indicated (Fig. 8a), but more contamination if a 12% partial melt of upper crust is used (Fig. 8b). In contrast, the Main Zone cumulates and B3 magma contain up to 50% by weight of a component of upper crustal residue.

Using Vredefort lower crust as the crustal end-member (Fig. 8c), up to 70% contamination would be indicated for the B1 magmas, which is inconsistent with the isotopic data.

Comparison between the Bushveld Complex and Continental Flood Basalts

In recent papers, Sharpe et al. (1986); Hatton (1995), and Hatton and Schweitzer (1995) have attributed Bushveld magmatism to melting in a mantle plume beneath the Kaapvaal Craton. The plume is thought to have provided the heat necessary to form the large volumes of high-degree mantle melts (Cox 1989; White and McKenzie 1989). The model suggests that the magmas parental to the complex were comparable to other large-scale continental magmatic provinces that are thought to be related to mantle plumes.

Continental flood basalt provinces show considerable compositional variation, but several examples in the literature have compositions similar to those inferred for Bushveld magmas, both in terms of incompatible trace elements (Fig. 9) and, in many cases, Sr and Nd isotopic signatures (not shown). The match is closest for those magmas in each volcanic province that contain the highest 'continental component', as expressed by high SiO_2 contents, highly enriched and strongly fractionated incompatible elements, large negative Nb–Ta anomalies, and 'enriched' isotopic compositions (high $^{87}Sr/^{86}Sr_i$ and low $\varepsilon Nd(T)$). Examples include the Nadezhdinsky member of the Siberian flood basalts (Lightfoot et al. 1990; Wooden et al. 1993), the Rajmahal Group II basalts of India (Kent et al. 1997), the Golden Gate unit of the Karoo basaltic province (Marsh et al. 1997), and the Mesozoic dolerite dykes of Tasmania (Hergt et al. 1989). An even better match is found with the marginal norites of the Muskox intrusion, which are believed to represent Coppermine River flood basalts contaminated in situ with partial melts of continental crust (Francis 1994). It is notable that the Nb–Ta and Ti depletion in Bushveld magmas is far more pronounced than in most flood basalts (Fig. 10), but that on the Kaapvaal Craton there are several examples of low-volume flood basalts that mimic the Nb–Ta and Ti depletion, amongst them the Klipriviersberg, Dominion Group (Marsh et al. 1989, 1992), and Rooiberg lavas (Hatton and Schweitzer 1995).

There is a parallel between up-section variations in trace-element ratios within the Bushveld Complex and changes within flood basalt sequences. The change from the strongly fractionated trace elements inferred for magmas in the lower part of the complex (e.g. B1-type sills) to the less fractionated patterns in the Main Zone (B3-type sills) is qualitatively similar to changes in volcanic sequences. For example, the Nadezhdinsky Formation of the Siberian flood basalts and the lower series of the Eskimo Formation of the Coppermine River basalts have far more fractionated patterns and higher concentrations of incompatible elements than basalts from overlying formations. In the volcanic sequences,

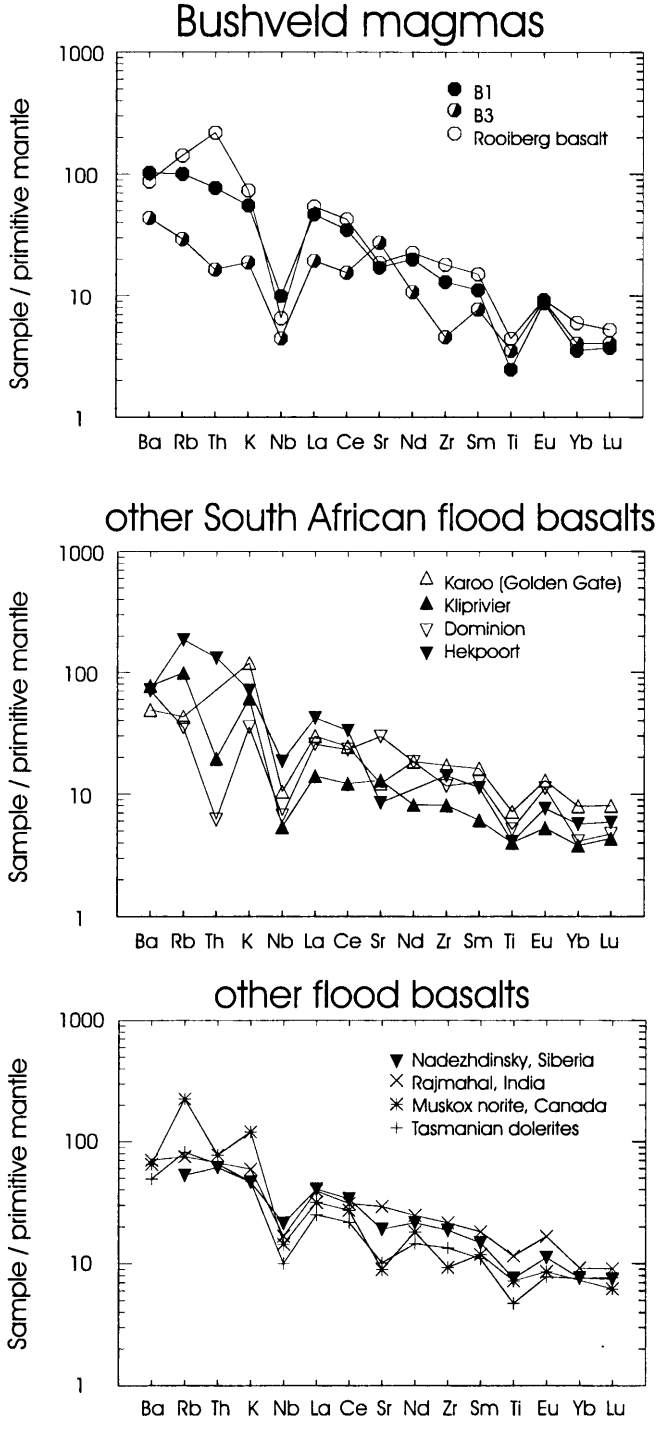

Fig. 9 Comparison between the trace-element compositions of selected flood basalts and magmas from the Bushveld Complex. Normalising values are from Sun and McDonough (1989)

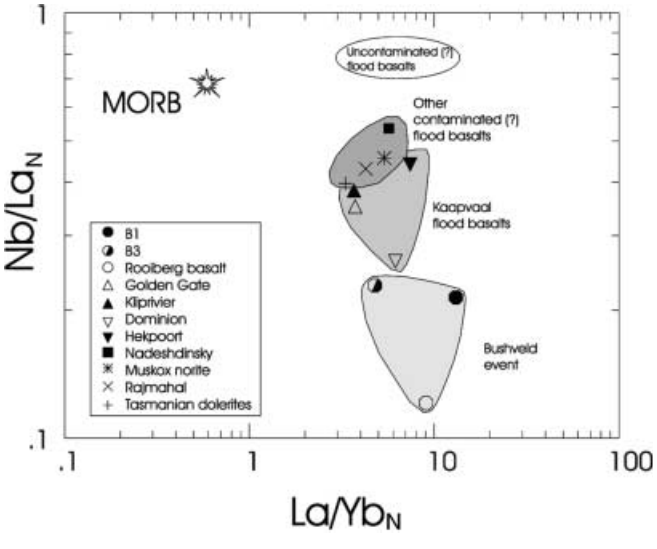

Fig. 10 Diagram of Nb/La_N vs La/Yb_N, comparing the composition of Bushveld magmas with those of other flood basalts and MORB. Normalising factors for primitive mantle are from Sun and McDonough (1989). Composition of MORB and uncontaminated(?) basalts (Snake River, Deccan, Parana) are from Wilson (1989)

however, the trace-element enrichment is accompanied by corresponding evolution in isotopic compositions: Sr isotope ratios are higher, and Nd isotope ratios are lower, in the Nadezhdinsky and lower Eskimo basalts than in the basalts from higher in the sequences. In other words, the volcanic sequences do not show the decoupling of trace-element and isotope ratios that distinguishes the Bushveld Complex. In the flood basalt sequences, the compositions of erupted magmas appear to have been controlled by variations of primary magma compositions and the extent of contamination with continental crust of relatively uniform composition. A pronounced change in contaminant composition, as inferred for the Bushveld Complex, seems not to have taken place.

The compositional similarity between Bushveld B1-type magmas and certain flood basalts raises the question as to whether there were any extrusive parts of the Bushveld Complex. Hatton and Schweitzer (1995) demonstrated the compositional similarity between basalts of the Rooiberg Group and B1 magmas (Fig. 9). Recent dating of the Rooiberg Group yielded ages between 2101–2060 m.y. (Walraven 1997), supporting a possible genetic link between the magmas. Compared with many other flood basalt provinces, the volume of extrusive basaltic rocks produced during the Bushveld event seems very small, but this may be because of deep erosion of Kaapvaal crust during the Cretaceous (Partridge 1998) or earlier.

Acknowledgements The authors would like to thank Nicole Morin, Joël Macé and Catherine Chauvel for their help in the isotope analytical work. The French–South African EARTH–ISE (Earth Sciences–International Scientific Exchange Project) financed the travel and accommodation and part of the analytical work. Other support was obtained from the CNRS GdR de Métallogénie. The samples were provided by Hugh Eales of Rhodes University. J.S. Marsh and R.E. Harmer made helpful comments on an earlier version of the manuscript. A.C. Kerr, I. Parsons and B.G.J. Upton are thanked for their critical reviews.

References

Arndt NT, Czamanske GK, Wooden JL, Fedorenko VA (1993) Mantle and crustal contributions to continental flood volcanism. Tectonophysics 223: 39–52

Arndt NT, Chauvel C, Fedorenko V, Czamanske G (1998) Two mantle sources, two plumbing systems: tholeiitic and alkaline magmatism of the Maymecha River basin, Siberian flood volcanic province. Contrib Mineral Petrol 133: 297–313

Buchanan PC, Koeberl C, Reimold WU (1999) Petrogenesis of the Dullstrom Formation, Bushveld magmatic province, South Africa. Contrib Mineral Petrol 137: 133–146

Condie KC (1993) Chemical composition and evolution of the upper continental crust: contrasting results from surface samples and shales. Chem Geol 104: 1–38

Cox KG (1989) The role of mantle plumes in the development of continental drainage patterns. Nature 342: 873–877

De Klerk WJ (1992) Petrogenesis of the Upper Critical Zone in the Western Bushveld Complex. PhD Thesis, Rhodes Univ, Grahamstown

DePaolo DJ (1981) Trace element and isotopic effects of combined wallrock assimilation and fractional crystallization. Earth Planet Sci Lett 53: 189–202

De Wit MJ, Roering C, Hart RJ, Armstrong RA, de Ronde CEJ, Green RWE, Tredoux M, Peberdy E, Hart RA (1992) Formation of an Archean continent. Nature 357: 553–562

Eales HV, De Klerk WJ, Butcher AR, Kruger FJ (1990) The cyclic unit beneath the UG1 chromitite (UG1FW unit) at RPM Union Section Platinum Mine. Mineral Mag 54: 23–43

Eales HV, Cawthorn RG (1996) The Bushveld Complex. In: Cawthorn RG (ed) Layered intrusions. Elsevier, Amsterdam, pp 181–229

Francis D (1994) Chemical interaction between picritic magmas and upper crust along the margins of the Muskox intrusion, Northwest Territories. Geol Soc Can, Pap 92–12

Francis DM, Hynes AJ (1979) Komatiite-derived tholeites in the Proterozoic of New Quebec. Earth Planet Sci Lett 44: 473–481

Hamilton PJ (1977) Sr isotope and trace element studies of the Great Dyke and Bushveld mafic phase and their relation to early Proterozoic magma genesis in South Africa. J Petrol 18: 24–52

Harmer RE, Sharpe MR (1985) Field relations and Sr isotope systematics of the marginal rocks of the Eastern Bushveld Complex. Econ Geol 80: 813–837

Harmer RE, von Gruenewaldt G (1991) A review of magmatism associated with the Transvaal Basin – implications for its tectonic setting. S Afr J Geol 94: 104–122

Harmer RE, Auret JM, Eglington BM (1995) Lead isotope variations within the Bushveld Complex, southern Africa: a reconnaissance study. J Afr Earth Sci 21: 595–606

Hart RJ, Welke HJ, Nicolaysen LO (1981) Geochronology of the deep profile through Archean basement at Vredefort, with implications for early crustal evolution. J Geophys Res 86(B11): 10663–10680

Hart RJ, Andreoli MAG, Tredoux M, De Wit MJ (1990) Geochemistry across an exposed section of Archaean crust at Vredefort, South Africa: with implications for mid-crustal discontinuities. Chem Geol 82: 21–50

Hart SR, Kinloch ED (1989) Osmium isotope systematics in Witwatersrand and Bushveld ore deposits. Econ Geol 84: 1651–1655

Hatton CJ (1995) Mantle plume origin for the Bushveld and Ventersdorp magmatic provinces. J Afr Earth Sci 21: 571–577

Hatton CJ (1996) The Bushveld Complex, a product of interaction among magmas derived from a mantle plume. Comm Geol Surv Namibia 10: 93–98

Hatton CJ, Sharpe MR (1989) Significance and origin of boninite-like rocks associated with the Bushveld Complex. In: Crawford AJ (ed) Boninites and related rocks. Unwin Hyman, London, pp 174–208

Hatton CJ, Schweitzer JK (1995) Evidence for synchronous extrusive and intrusive Bushveld magmatism. J Afr Earth Sci 21: 579–594

Hergt JM, Chappell BW, McCulloch MT, McDougall I, Chivas AR (1989) Geochemical and isotopic constraints on the origin of the Jurassic dolerites of Tasmania. J Petrol 39: 841–883

Irvine TN (1970) Crystallization sequences in the Muskox intrusion and other layered intrusions. 1. Olivine–pyroxene–plagioclase relations. Geol Soc S Afr, Spec Publ 1: 441–476

Kent W, Saunders AD, Kempton PD, Ghose NC (1997) Rajmahal basalts, eastern India: Mantle sources and melt distribution at a volcanic rifted margin. In: Mahoney JJ, Coffin MF (eds) Large igneous provinces. Geophys Monogr 100, Am Geophys Union, pp 145–182

Kerr AC, Kempton PD, Thompson RN (1995) Crustal assimilation during turbulent magma ascent (ATA); new isotopic evidence from the Mull Tertiary lava succession, NW Scotland. Contrib Mineral Petrol 119: 142–154

Kruger FJ (1994) The Sr-isotopic stratigraphy of the Western Bushveld Complex. S Afr J Geol 97: 393–398

Lambert DD, Walker RJ, Morgan JW, Shirey SB, Carlson RW, Zientek ML, Lipin BR, Koski MS, Cooper RL (1994) Re–Os and Sm–Nd isotope geochemistry of the Stillwater Complex, Montana: implications for the petrogenesis of the J-M reef. J Petrol 35: 1717–1753

Lassiter JC, DePaolo DJ (1997) Plume/lithosphere interaction in the generation of continental and oceanic flood basalts: chemical and isotopic constraints. In: Mahoney JJ, Coffin MF (eds) Large igneous provinces. Geophys Monogr 100, Am Geophys Union, pp 335–356

Lightfoot PC, Naldrett AJ, Gorbachev NS, Doherty W, Fedorenko VA (1990) Geochemistry of the Siberian Trap of the Noril'sk area, USSR, with implications for the relative contributions of crust and mantle to flood basalt magmatism. Contrib Mineral Petrol 104: 631–644

Maier WD, Barnes S-J (1998) Concentrations of rare earth elements in silicate rocks of the Lower, Critical and Main Zones of the Bushveld Complex. Chem Geol 150: 85–103

Maier WD, Barnes S-J (1999) Platinum-group elements in silicate rocks of the Lower, Critical and Main Zones at Union Section, Western Bushveld Complex. J Petrol 40: 1647–1671

Marsh JS, Bowen MP, Rogers NW, Bowen TB (1989) Volcanic rocks of the Witwatersrand Triad, South Africa, I: petrogenesis of mafic and felsic rocks of the Dominion Group. Precambrian Res 44: 39–65

Marsh JS, Bowen MP, Rogers NW, Bowen TB (1992) Petrogenesis of Late Archean flood-type basic lavas from the Klipriviersberg group, Ventersdorp Supergroup, South Africa. J Petrol 33: 817–847

Marsh JS, Hooper PR, Rehacek J, Duncan RA, Duncan AR (1997) Stratigraphy and age of Karoo basalts of Lesotho and implications for correlations within the Karoo igneous province. In: Mahoney JJ, Coffin MF (eds) Large igneous provinces. Geophys Monogr 100, Am Geophys Union, pp 247–272

McCandless TE, Ruiz J, Adair BI, Freydier C (1999) Re–Os and Pd/Ru variations in chromitites from the Critical Zone, Bushveld Complex, South Africa. Geochim Cosmochim Acta 63: 911–923

Mitchell AA (1986) The petrology, mineralogy, and geochemistry of the Main Zone of the Bushveld Complex at Rustenburg Platinum Mines, Union Section. PhD Thesis, Rhodes Univ, Grahamstown

O'Hara MJ, Mathews RE (1981) Geochemical evolution in an advancing, periodically replenished, periodically tapped, continuously fractionated magma chamber. J Geol Soc Lond 138: 237–277

Partridge TC (1998) Of diamonds, dinosaurs and diastrophism: 150 million years of landscape evolution in southern Africa. S Afr J Geol 101: 165–184

Patiño Douce AE, Beard JS (1995) Dehydration-melting of biotite gneiss and quartz amphibolite from 3 to 15 kbar. J Petrol 36: 707–738

Plank T, Langmuir CH (1998) The chemical composition of subducting sediment and its consequences for the crust and mantle. Chem Geol 145: 325–394

Rudnick RL, Fountain DM (1995) Nature and composition of the continental crust: a lower crust perspective. Rev Geophys 33: 267–309

Rudnick RL, Presper T (1990) Geochemistry of intermediate to high-pressure granulites. In: Vielzeuf D, Vidal P (eds) Granulites and crustal evolution. Kluwer, Amsterdam, pp 523–550

Schoenberg R, Kruger FJ, Kramers JD (1998) The formation of the PGE bearing Bushveld chromitites and the Merensky Reef by magma mixing: a combined Re–Os and Rb–Sr study. (Abstr) Goldschmidt Conf, Toulouse, Mineral Mag 62A: 1349–1350

Sharpe MR (1978) 'Cone-type' diabases from the eastern Transvaal – representatives of a quenched magma. Geol Soc S Afr Trans 81: 373–378

Sharpe MR (1981) The chronology of magma influxes to the eastern compartment of the Bushveld Complex as exemplified by its marginal border group. J Geol Soc 138: 307–326

Sharpe MR, Irvine TN (1983) Melting relations of two Bushveld chilled margin rocks and implications for the origin of chromitite. Carnegie Inst Wash Year Book 82: 295–300

Sharpe MR, Evensen NM, Naldrett AJ (1986) Sm/Nd and Rb/Sr evidence for liquid mixing, magma generation and contamination in the Eastern Bushveld Complex. In: Geocongress, Conf Abstr, University of the Witwatersrand, Johannesburg, pp 621–624

Sparks RSJ (1986) The role of crustal contamination in magma evolution through geological time. Earth Planet Sci Lett 78: 211–223

Stewart BM, de Paolo DJ (1990) Isotopic studies of processes in mafic magma chambers: II. The Skaergaard Intrusion, East Greenland. Contrib Mineral Petrol 104: 125–141

Sun S-S, McDonough WF (1989) Chemical and isotopic systematics of oceanic basalts: implications for mantle composition and processes. In: Saunders AD, Norry MJ (eds) Magmatism in the ocean basins, Spec Publ 42, Geol Soc, Oxford, pp 313–345

Taylor SR, McLennan SM (1985) The continental crust: its composition and evolution. Blackwell, Oxford

Teigler B, Eales HV (1996) The lower and critical zones of the western limb of the Bushveld Complex as intersected by the Nooitgedacht boreholes. Geol Surv S Afr Bull, no 111

Walraven F (1997) Geochromology of the Rooiberg Group, Transvaal Supergroup, South Africa. Econ Geol Res Unit Inform Circ 316, University of the Witwatersrand, Johannesburg

Walraven F, Armstrong RA, Kruger FJ (1990) A chronostratigraphic framework for the north-central Kaapvaal craton, the Bushveld Complex and the Vredefort structure. Tectonophysics 171: 23–48

White RW, McKenzie DP (1989) Magmatism at rift zones: the generation of volcanic continental margins and flood basalts. J Geophys Res 94: 7685–7729

Wilson M (1989) Igneous petrogenesis. Chapman and Hall, London

Wooden JL, Czamanske GK, Fedorenko VA, Arndt NT, Chauvel C, Bouse RM, King BW, Knight RJ, Siems DF (1993) Isotopic and trace element constraints on mantle and crustal contributions to Siberian continental flood basalts, Noril'sk area, Siberia. Geochim Cosmochim Acta 57: 3677–3704